Bioorganic & Medicinal Chemistry xxx (2015) xxx–xxx

Contents lists available at ScienceDirect

Bioorganic & Medicinal Chemistry

journal homepage: www.elsevier.com/locate/bmc

Chimeric derivatives of functionalized amino acids and α-aminoamides: Compounds with anticonvulsant activity in seizure models and inhibitory actions on central, peripheral, and cardiac isoforms of voltage-gated sodium channels

Robert Torregrosa [a], Xiao-Fang Yang [b], Erik T. Dustrude [c], Theodore R. Cummins [c,d], Rajesh Khanna [b,*], Harold Kohn [a,e,f,*]

[a] NeuroGate Therapeutics, Inc., 150 Fayetteville Street, Suite 2300, Raleigh, NC 27601, United States
[b] Department of Pharmacology and Neuroscience Graduate Interdisciplinary Program, College of Medicine, University of Arizona, Tucson, AZ 85742, United States
[c] Program in Medical Neuroscience, Paul and Carole Stark Neurosciences Research Institute, Indiana University School of Medicine, Indianapolis, IN 46202, United States
[d] Department of Pharmacology and Toxicology, Indiana University School of Medicine, Indianapolis, IN 46202, United States
[e] Division of Chemical Biology and Medicinal Chemistry, UNC Eshelman School of Pharmacy, University of North Carolina, Chapel Hill, NC 27599, United States
[f] Department of Chemistry, University of North Carolina, Chapel Hill, NC 27599, United States

ARTICLE INFO

Article history:
Received 30 January 2015
Revised 26 March 2015
Accepted 3 April 2015
Available online xxxx

Keywords:
Chimeric agents
Functionalized amino acids
α-Aminoamides
Antiseizure agents
Na^+ current inhibition

ABSTRACT

Six novel 3″-substituted (*R*)-*N*-(phenoxybenzyl) 2-*N*-acetamido-3-methoxypropionamides were prepared and then assessed using whole-cell, patch-clamp electrophysiology for their anticonvulsant activities in animal seizure models and for their sodium channel activities. We found compounds with various substituents at the terminal aromatic ring that had excellent anticonvulsant activity. Of these compounds, (*R*)-*N*-4′-((3″-chloro)phenoxy)benzyl 2-*N*-acetamido-3-methoxypropionamide ((*R*)-**5**) and (*R*)-*N*-4′-((3″-trifluoromethoxy)phenoxy)benzyl 2-*N*-acetamido-3-methoxypropionamide ((*R*)-**9**) exhibited high protective indices (PI = TD_{50}/ED_{50}) comparable with many antiseizure drugs when tested in the maximal electroshock seizure test to mice (intraperitoneally) and rats (intraperitoneally, orally). Most compounds potently transitioned sodium channels to the slow-inactivated state when evaluated in rat embryonic cortical neurons. Treating HEK293 recombinant cells that expressed $hNa_V1.1$, $rNa_V1.3$, $hNa_V1.5$, or $hNa_V1.7$ with (*R*)-**9** recapitulated the high levels of sodium channel slow inactivation.

1. Introduction

The epilepsies are serious, neurological disorders that affect up to 1% of the world's population.[1] Although more than 40 drugs have been used to treat these disorders,[2] significant health needs remain unmet. First, current antiseizure drugs (ASDs) are ineffective for about one-third of patients, even when multiple drugs are prescribed.[3] Second, ASD use is associated with untoward side effects in more than 40% of patients, ranging from common cosmetic (e.g., gingival hyperplasia, weight gain) and quality of life (e.g., sedation, learning, cognitive dysfunction) to rare, life-threatening (e.g., hepatotoxicity, aplastic anemia) ones.[4,5] Third, some epilepsies, such as Lenox-Gestault and mesial temporal lobe epilepsy, worsen over time, and for these disorders, there is a need for a disease-modifying drug.[6] Finally, most seizure medications do not address associated comorbidities (e.g., cognitive dysfunction[7]). Thus, the need still remains for ASDs that have novel mechanism(s) of action with safe profiles.

We have reported on a novel series of chimeric compounds, (*R*)-**A**,[8–10] derived from the merger of key structural units (Fig. 1B, **C**) present in the functionalized amino acid (FAA), lacosamide[11] ((*R*)-*N*-benzyl 2-*N*-acetamido-3-methoxypropionamide, (*R*)-**1**) and the α-aminoamide (AAA), safinamide[12,13]

Abbreviations: AAA, α-aminoamide; ASD, antiseizure drug; ASP, Anticonvulsant Screening Program; CAD, catecholamine A-differentiated; CNS, central nervous system; ED_{50}, effective dose (50%); FAA, functionalized amino acid; IBCF, isobutyl chloroformate; IC_{50}, concentration at which half of the channels have transitioned to a slow-inactivated state; ip, intraperitoneally; MAC, mixed anhydride coupling; MES, maximal electroshock seizure; NINDS, National Institutes of Neurological Disorders and Stroke; NMM, *N*-methylmorpholine; NOAEL, no observed adverse effect level; OCF_3, trifluoromethoxy; PI, protective index; po, orally; RMP, resting membrane potential; SAR, structure activity relationship; scMet, scMetrazol; TD_{50}, neurological impairment (toxicity, 50%); TEA-Cl, tetraethylammonium chloride; $V_{1/2}$, voltage of half-maximal (in)activation; VGSC, voltage-gated sodium channel.

* Corresponding authors.

http://dx.doi.org/10.1016/j.bmc.2015.04.014
0968-0896/

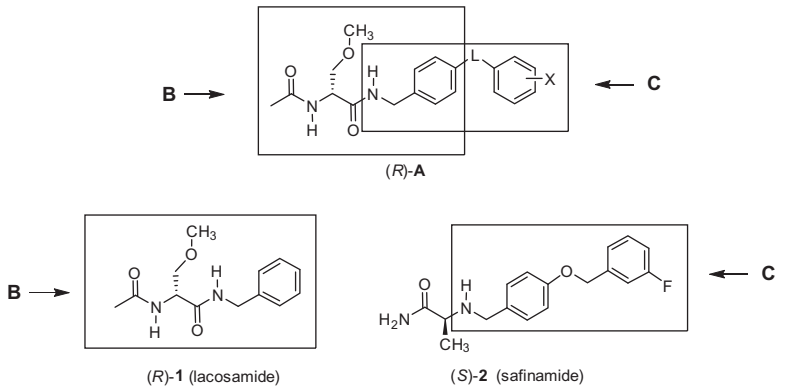

Figure 1. Generation of chimeric class (*R*)-**A** from (*R*)-**1** and (*S*)-**2**. Box B represents lacosamide ((*R*)-**1**) and Box C represents safinamide ((*S*)-**2**) derived component.

((*S*)-2-(4′-((3″-fluoro)benzyloxy)benzyl)aminopropionamide, (*S*)-**2**). Lacosamide is a first-in-class ASD that is extensively used for the treatment of partial-onset seizures in adults.[14] Safinamide, another anticonvulsant,[15] has been advanced for the treatment of Parkinson's disease.[16] Studies have shown that safinamide inhibits monoamine oxidase type B,[17] thus likely preventing dopamine bioactivation in patients suffering from Parkinson's disease. We demonstrated that select (*R*)-**A** compounds displayed potent anticonvulsant activities in the maximal electroshock[18] (MES) and the 6-Hz psychomotor[19] seizure assays in rodents.[8–10] The anticonvulsant activities of (*R*)-**A** have been attributed, in part, to their actions on voltage-gated sodium channel (VGSC) properties.[9,10,20] Chimeric compounds (*R*)-**A** potently transitioned VGSCs to the slow-inactivated state and in some cases, affected fast inactivation processes and inhibited Na^+ currents in a frequency (use)-dependent fashion. The experimental findings for slow inactivation by (*R*)-**A** were also consistent with a mechanism in which the chimeric compounds block fast-inactivated channels with very slow kinetics.[21,22]

An initial structure–activity relationship (SAR) study of (*R*)-**A** showed excellent anticonvulsant activities for compounds in which the two aryl units were in spatial proximity.[8] Thus, we further investigated the activities of (*R*)-**A** compounds wherein the linker (L) was either a single bond[9] or an oxymethylene (OCH_2)[10] group and found that the X-substituent in the terminal aromatic ring influenced the cellular and whole animal pharmacological activities. Here, we explore the (*R*)-**A** series that contain an oxy (O)-linker to give (*R*)-**D**. We demonstrate in seizure models that most X-substituents in (*R*)-**D** yielded compounds with excellent anticonvulsant activities and minimal neurotoxicities, comparable with many ASDs. Electrophysiology studies showed that (*R*)-**D** displayed sodium channel properties consistent with other members of this general class of compounds.[9,10,20]

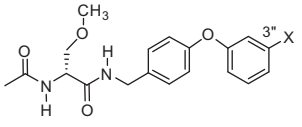

(*R*)-**D**

2. Results

2.1. Selection of compounds

We prepared compounds (*R*)-**3** and (*R*)-**5**–(*R*)-**9** where an oxygen was the linker (L) between the two aromatic rings. Our initial SAR study documented that (*R*)-**4**, the 3″-fluorine (*R*)-**D** derivative, exhibited pronounced anticonvulsant activity in rodents.[8] Accordingly, we restricted the site of substitution on the terminal aromatic ring to the 3″-position. The X-substituent ranged from electron-withdrawing to electron-donating groups.

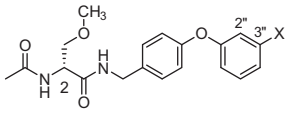

(*R*)-**3**; X = H
(*R*)-**4**; X = F
(*R*)-**5**; X = Cl
(*R*)-**6**; X = CH_3
(*R*)-**7**; X = CF_3
(*R*)-**8**; X = OCH_3
(*R*)-**9**; X = OCF_3

2.2. Synthesis

Compounds (*R*)-**3** and (*R*)-**5**–(*R*)-**9** were prepared by a similar route (Scheme 1), using the mixed anhydride coupling (MAC) method.[23] Commercially available (*R*)-*N*-*tert*-butoxycarbonyl-D-serine ((*R*)-**27**) was coupled with the 4-(phenoxy)phenylmethamines **21**–**26** using the MAC reagents isobutylchloroformate (IBCF) and *N*-methylmorpholine (NMM) to give amides (*R*)-**28**–(*R*)-**33**, respectively, without racemization of the C(2) chiral center. The substituted 4-phenoxybenzylamines were prepared by treating 4-fluorobenzonitrile (**10**) with the appropriate aryl phenol (**11**–**15**) using either K_2CO_3 or Cs_2CO_3 in DMF to give the corresponding nitriles.[24–27] Subsequent reduction of the nitrile group in **16**–**20** with $LiAlH_4$ afforded the amines **22**–**26**. The corresponding unsubstituted 4-phenoxybenzylamine (**21**) was commercially available. Methylation (CH_3I, Ag_2O) of the serine hydroxyl group in (*R*)-**28**–(*R*)-**33** provided ethers (*R*)-**34**–(*R*)-**39**, respectively. Deprotection of the *tert*-butoxycarbonyl group in (*R*)-**34**–(*R*)-**39** with acid (HCl/dioxane) followed by acetylation (AcCl, Et_3N) gave the desired products (*R*)-**3** and (*R*)-**5**–(*R*)-**9**, respectively. The enantiomeric purities of (*R*)-**3** and (*R*)-**5**–(*R*)-**9** were assessed by the detection of a single acetyl methyl peak and a single *O*-methyl peak in the ^1H NMR spectrum for each compound when a saturated solution of (*R*)-(−)-mandelic acid was added.[28]

We report, in the Section 5, the details (synthetic procedure, characterization) of the final step for all compounds evaluated in the seizure and cellular electrophysiology studies. In the Supporting information, we provide the experimental procedures and the physical and full spectroscopic properties for all the synthetic compounds prepared in this study.

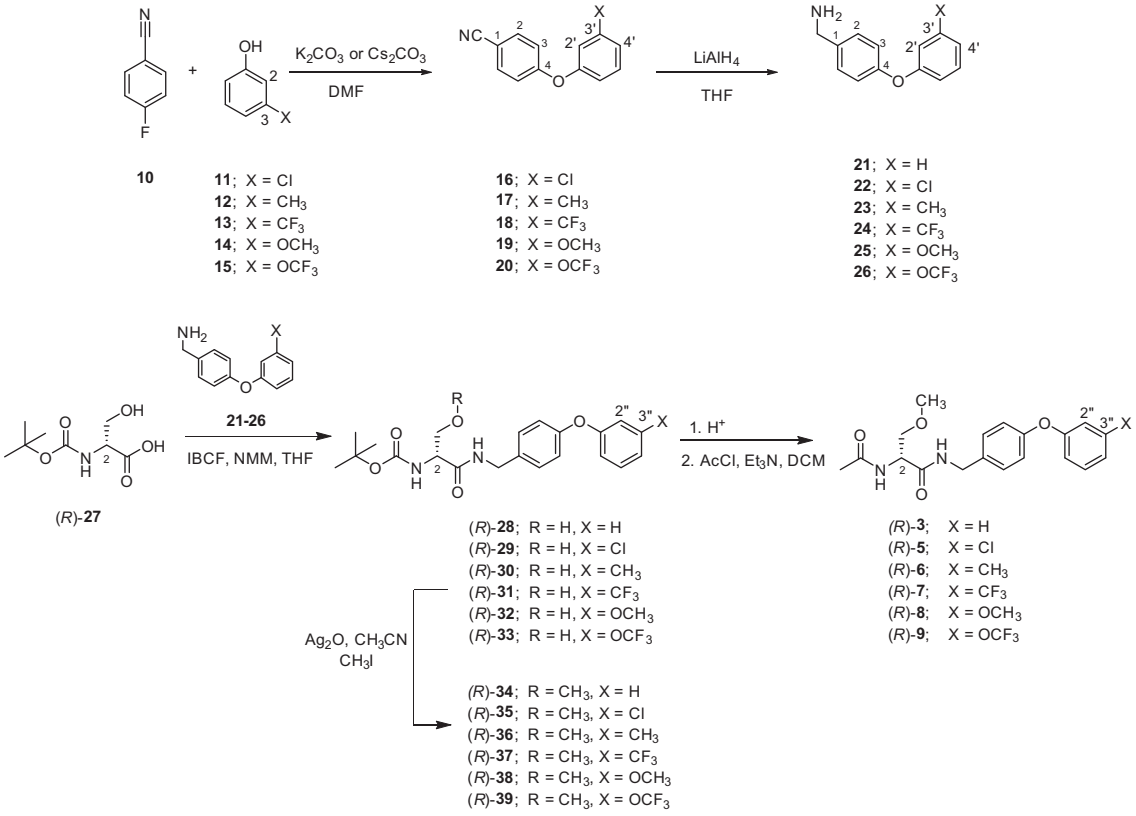

Scheme 1. Synthesis of (*R*)-**3** and (*R*)-**5**–(*R*)-**9**.

2.3. Pharmacological evaluation

2.3.1. Whole animal pharmacological activity

Compounds (*R*)-**3** and (*R*)-**5**–(*R*)-**9** were tested for anticonvulsant activity at the Anticonvulsant Screening Program (ASP) of the National Institute of Neurological Disorders and Stroke (NINDS), U.S. National Institutes of Health, using the procedures described by Stables and Kupferberg.[29] The anticonvulsant data from the MES model[18] (mice, intraperitoneally (ip); rat, ip; rat, orally (po)), and the psychomotor 6 Hz (32 mA) seizure test for therapy-resistant limbic seizures[19] (mice, ip) are summarized in Table 1 along with similar results (where available) obtained for (*R*)-**1**,[11,30] (*S*)-**2**,[15] and (*R*)-**4**,[8] and the ASDs phenytoin,[31,32] phenobarbital,[31] and valproate.[31] For compounds that showed significant activity, we report the 50% effective dose (ED_{50}) values from quantitative screening evaluations. We also include the median doses for 50% neurological impairment (TD_{50}) in mice, using the rotorod test,[33] and the behavioral toxicity effects observed in rats.[34] The protective index ($PI = TD_{50}/ED_{50}$) for the test compounds is listed, where possible. Compounds (*R*)-**4**–(*R*)-**6**, (*R*)-**8** and (*R*)-**9** were evaluated in the subcutaneous Metrazol (scMet) seizure model,[35] and no activity was observed below 40 mg/kg (data not shown). Similarly, we found no activity in the scMet model for (*R*)-**1**[11] and structurally related compounds.[8–10,36]

Compounds (*R*)-**3**–(*R*)-**9** displayed excellent activities in the MES model in mice when administered ip and in rats when administered either ip or po. For most compounds, we observed in mice (ip) ED_{50} values that ranged from 5.5 to 14 mg/kg, values that were comparable with the ASDs (*R*)-**1**[11] and phenytoin[31,32] (ED_{50} (mg/kg): (*R*)-**3**, >10, <30; (*R*)-**4**, 5.5; (*R*)-**5**, 9.4; (*R*)-**6**, 14; (*R*)-**7**, ~10; (*R*)-**8**, 13; (*R*)-**9**; 6.5; (*R*)-**1**, 4.5; phenytoin, 9.5). Furthermore, we found that many of the compounds exhibited low neurotoxicities in the rotorod test in mice (ip), thus affording high PI values similar to (*R*)-**1**[11] and phenytoin[31,32] (PI: (*R*)-**4**, 4.2; (*R*)-**5**, 5.0; (*R*)-**6**, 4.6; (*R*)-**8**, 6.5; (*R*)-**9**, 6.2; (*R*)-**1**, 6.0; phenytoin, 6.9). In rats (po), excellent activities were observed for (*R*)-**5** and (*R*)-**9** (ED_{50} (mg/kg): (*R*)-**5**, 12; (*R*)-**9**, 8.3). The PI values for these compounds were high but were lower than (*R*)-**1** and phenytoin (PI: (*R*)-**5**, 18; (*R*)-**9**, 29; (*R*)-**1**, >130; phenytoin, >36). In rats (ip), (*R*)-**5**, (*R*)-**6**, (*R*)-**8**, and (*R*)-**9** displayed potent activities (ED_{50} values: 5.7–15 mg/kg) and low neurotoxicities (TD_{50} values: 49–140 mg/kg) giving PI values that ranged from 8.0 to 12, values higher than phenytoin[32] (PI: (*R*)-**5**, 8.3; (*R*)-**6**, 12; (*R*)-**8**, 8.0; (*R*)-**9**, 9.5; phenytoin, 6.3). Finally, we evaluated (*R*)-**3**–(*R*)-**9** in the 6 Hz (32 mA) psychomotor seizure test and found that (*R*)-**4**, (*R*)-**5**, and (*R*)-**9** were the most active compounds (ED_{50} (mg/kg): (*R*)-**4**, ~10; (*R*)-**5**, 20; (*R*)-**9**, 15). By comparison, the 6 Hz ED_{50} value for (*R*)-**1** was 10 mg/kg.[30]

2.3.2. Whole-cell, patch-clamp electrophysiological activity

The well-described mechanisms of action by lacosamide and safinamide, parents of (*R*)-**D** series compounds, both involve inhibition of VGSCs.[14,15,37,38] Promising anticonvulsant activities of (*R*)-**3**–(*R*)-**9** therefore prompted our examination of the VGSC activities in rat embryonic cortical neurons[9,10,39] by whole-cell, patch-clamp electrophysiology. These neurons typically express central nervous system (CNS) sodium channel isoforms $Na_V1.1$, $Na_V1.2$, $Na_V1.3$, and $Na_V1.6$.[40] Kinetic properties of slow inactivation, frequency (use)-dependence, steady-state activation, and fast inactivation of Na^+ currents were measured in the presence of (*R*)-**3**–(*R*)-**9**. The cortical neurons were grown for 7–10 days in vitro and then examined using protocols described earlier.[9,10,39] Compounds (*R*)-**3**–(*R*)-**9** were tested only at 10 μM due to constraints of cortical neuron viability during the course of the patch-clamp experiments. Here, we did not separate the exact contribution of the four Na_v isoforms in the presence of (*R*)-**3**–(*R*)-**9** because of the lack of subtype-specific blockers of these Na_v

Table 1
Structure–activity relationship for chimeric compounds (*R*)-**D**[a]

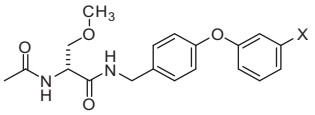

Compd No.	X	Mice[b] (ip)				Rat[g] (po)			Rat[b] (ip)		
		MES[c] ED_{50} (mg/kg)	6 Hz[d] ED_{50} (mg/kg)	Tox[e] TD_{50} (mg/kg)	PI[f]	MES[c] ED_{50} (mg/kg)	Tox[h] TD_{50} (mg/kg)	PI[f]	MES[c] ED_{50} (mg/kg)	Tox[h] TD_{50} (mg/kg)	PI[f]
(*R*)-**3**	H	>10, <30 [0.5–2.0]	>10, <30 [0.5]	>30, <100 [0.5]	–	ND[i]	ND[i]	–	ND[i]	ND[i]	–
(*R*)-**4**[j]	F	5.5 [0.25] (3.2–6.3)	~10 [0.25–0.5]	23 [0.25] (18–28)	4.2	<10 [0.25–4.0]	>10 [0.25–4.0]	–	ND[i]	ND[i]	–
(*R*)-**5**	Cl	9.4 [0.5] (7.6–11)	20 [0.25] (15–25)	47 [0.25] (42–51)	5.0	12 [1.0] (6.9–18) [1.0–2.0]	210 [0.5] (200-250)	18	5.9 [0.5] (3.7–7.9)	49 [0.5] (34–61)	8.3
(*R*)-**6**	CH_3	14 [0.25] (11–17)	~100 [0.5]	65 [0.25] (57–73)	4.6	<30 [0.5]	>30 [0.25–4.0]	–	12 [0.25] (10–13)	140 [0.25] (90–190)	12
(*R*)-**7**	CF_3	~10 [0.5]	>10, <100 [0.5]	>100 [0.5]	–	<30 [0.5–4.0]	>30 [0.25–4.0]	–	ND[i]	ND[i]	–
(*R*)-**8**	OCH_3	13 [0.25] (12–14)	>30, <100 [0.5]	85 [0.25] (75–100)	6.5	~30 [0.25–1.0]	>30 [0.25–4.0]	–	15 [0.25] 8.0–21)	120 [1] (86–150)	8.0
(*R*)-**9**	OCF_3	6.5 [0.25] (5.1–8.2)	15 [0.25] (9.1–22)	40 [0.25] (36–45)	6.2	8.3 [2.0] (4.9–11)	240 [1.0] (160–390)	29	5.7 [2.0] (3.6–7.8)	54 [2.0] (40–66)	9.5
(*R*)-**1**[k,l]		4.5 [0.5] (3.7–5.5)	10 [0.5] (7.8–13)	27 [0.25] (26–28)	6.0	3.9 [2.0] (2.6–6.2)	>500 [0.5]	>130	NA[m]	NA[m]	–
(*S*)-**2**[n]		4.1 (3.0–5.5)				12 (10–14)			NA[m]	NA[m]	–
Phenytoin[o,p]		9.5 [2.0] (8.1–10)		66 [2.0] (53–72)	6.9	28 (21–35)	>1000	>36	2.4 (1.4–3.7)	15 (12–19)	6.3
Phenobarbital[o]		22 [1.0] (15–23)		69 [0.5] (63–73)	3.2	9.1 [5.0] (7.6–12)	61 [0.5] (44–96)	6.7	NA[m]	NA[m]	–
Valproate[o]		270 [0.25] (250–340)		430 [0.25] (370–450)	1.6	490 [0.5] (350–730)	280 [0.5] (190–350)	0.6	NA[m]	NA[m]	–

[a] The compounds were tested through the NINDS ASP.
[b] The compounds were administered intraperitoneally. ED_{50} and TD_{50} values are in milligrams per kilogram.
[c] MES = maximal electroshock seizure test. Numbers in parentheses are 95% confidence intervals. A dose–response curve was generated for all compounds that displayed sufficient activity. The dose–effect for these compounds was obtained at the 'time of peak effect' (indicated in hours in the brackets).
[d] 6 Hz = 6 Hz (32 mA) psychomotor seizure test.
[e] TD_{50} value determined from the rotorod test.
[f] PI = protective index (TD_{50}/ED_{50}).
[g] The compounds were administered orally. ED_{50} and TD_{50} values are in milligrams per kilogram. Numbers in parentheses are 95% confidence intervals. A dose–response curve was generated for all compounds that displayed sufficient activity. The dose–effect for these compounds was obtained at the 'time of peak effect' (indicated in hours in the brackets).
[h] Tox = behavioral toxicity.
[i] ND = not determined.
[j] Ref. 8.
[k] Ref. 11.
[l] Ref. 30.
[m] NA = data not available.
[n] Ref. 15.
[o] Ref. 31.
[p] Ref. 32.

isoforms, and the possible interactions between said blockers of various Na_V channels and the (*R*)-**D** compounds themselves. Thus, we assumed contributions from all four CNS Na_V isoforms. The excellent anticonvulsant activity observed for (*R*)-**9** led us to examine this compound further in both catecholamine A-differentiated (CAD) cells[41] that express predominantly $Na_v1.7$ and in recombinant HEK293 cells that express $hNa_V1.1$, $rNa_V1.3$, $hNa_V1.5$, or $hNa_V1.7$ channels.[9]

2.3.2.1. Rat embryonic cortical neurons. First, we tested the ability of 10 μM (*R*)-**3**–(*R*)-**9** to modulate the transition of VGSCs to a slow-inactivated state. Cortical cells were conditioned to potentials ranging from −100 mV to +20 mV (in +10 mV increments) for 5 s.[9,39,42] Channels that underwent fast inactivation during this conditioning pulse were then allowed to recover during a 1 s pulse to −70 mV before the extent of slow inactivation was examined by a test pulse to −10 mV, for 20 ms (Fig. 2A, left). Representative traces illustrating the extent of slow inactivation observed at −50 mV compared to the prepulse at −100 mV in the absence (control) or presence of (*R*)-**5** and (*R*)-**8** are shown in Figure 2A (*right*), with the full slow inactivation curve (normalized peak versus prepulse potential) of (*R*)-**5** shown in Figure 2B. At 10 μM, (*R*)-**5** facilitated the transition of a majority of sodium channels into the slow-inactivated state compared with control (0.1% DMSO)-treated neurons. Slow inactivation at −50 mV was chosen as a point of comparison between compounds due to the physiological relevance of this voltage near the resting membrane potential and action potential firing threshold of neurons. At this voltage, VGSC activation and inactivation kinetics mediate channel availability that determines if sustained firing, akin to that during an epileptic

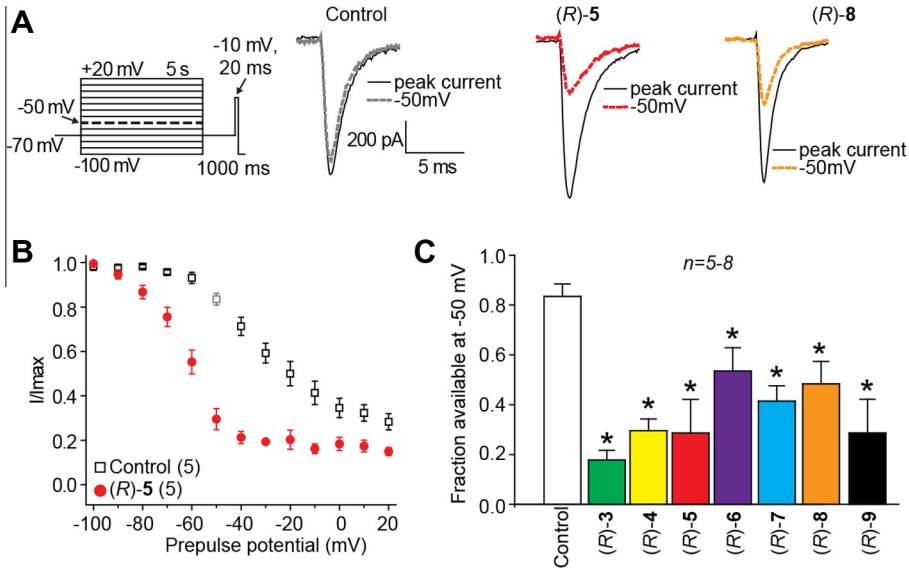

Figure 2. Effects of (*R*)-**3**–(*R*)-**9** on steady-state slow inactivation state of Na^+ currents in embryonic cortical neurons. (A) Voltage protocol for slow inactivation. Currents were evoked by 5 s prepulses between −100 mV and +20 mV (in 10 mV increments), and then fast-inactivated channels were allowed to recover for 1000 ms at a hyperpolarized pulse to −70 mV before testing for the fraction of available channels for 20 ms at −10 mV. The fraction of channels available at −10 mV was analyzed. Representative current traces from cortical neurons in the absence (control, 0.1% DMSO) or presence of 10 μM (*R*)-**5** or (*R*)-**8** are illustrated. The black and dashed traces represent the currents evoked at −100 and −50 mV, respectively (also highlighted in the voltage protocol as a dashed line). (B) Summary of steady-state slow activation curves for neurons treated with DMSO (control) or 10 μM (*R*)-**5**. Significant drug-induced slow inactivation was evident at voltages more depolarizing than −80 mV in neurons treated with (*R*)-**5**. (C) Summary of the fraction of current available at −50 mV for neurons treated with 0.1% DMSO (control) or 10 μM of the indicated compounds. Asterisks (*) indicate statistically significant differences in fraction of current available between control and the indicated compounds (p <0. 05, Student's t-test). Data are from 5 to 8 cells per condition.

event, is possible.[43–47] At −50 mV, a small fraction (i.e., 0.16 ± 0.05 n = 5; calculated as 1 minus the normalized I_{Na}) of the channels had entered a slow-inactivated conformational state(s) in control-treated cells (Fig. 2B and C). Compared with the control, (*R*)-**3**–(*R*)-**9** caused a significant decrease in the maximal fraction of current that is available by depolarization, with maximal induction observed in the presence of (*R*)-**3** (0.82 ± 0.03, n = 5) (p <0.01, Mann–Whitney U test).

We next interrogated if (*R*)-**3**–(*R*)-**9** could enhance steady-state fast inactivation. For these studies we used a similar protocol (Fig. 3, *top left*) designed to induce a fast-inactivated state.[9] Cells were subjected to inactivating prepulse potentials ranging from −100 to −10 mV (in 10-mV increments) for 500 ms prior to a 0 mV test pulse for 20 ms to estimate the extent of fast inactivation. The 500 ms conditioning pulse allows for examination of the linear range of fast inactivation curves for endogenous channels at assayed potentials. Steady-state, fast inactivation curves of Na^+ currents from control (0.1% DMSO)- and (*R*)-**3**–(*R*)-**9**–treated cortical neurons were well fitted with a single Boltzmann function (R^2 >0.963 for all conditions). The value of voltage of half-maximal inactivation ($V_{1/2}$) for 0.1% DMSO-treated cells was −53.4 ± 1.5 mV (n = 4), which was not significantly different from that observed for (*R*)-**3**–(*R*)-**9** (p >0.05 vs control; Student's t-test; Fig. 3).

Next, we tested whether (*R*)-**3**–(*R*)-**9** could alter the voltage-dependence of activation for cortical neuron VGSCs. Activation changes for cortical neurons treated with compounds were measured by whole-cell ionic conductances in response to changes in command voltage (Fig. 3, *top right*) and analyzed by comparing Boltzmann properties of half maximal activation ($V_{1/2}$) and slope factors (k).[9,39] Boltzmann fits for 0.1% DMSO (control) and (*R*)-**3**–(*R*)-**9** are shown in Figure 3. The $V_{1/2}$ value for steady-state activation for 0.1% DMSO-treated (control) neurons was −27.1 ± 1.3 mV (n = 5), which was significantly different from that of (*R*)-**7** (−35.6 ± 4.1 mV; n = 5) and (*R*)-**8** (−36.8 ± 1.0 mV; n = 6) (p <0.05 vs control; Student's t-test; Fig. 3) but not for (*R*)-**3**–(*R*)-**6** and (*R*)-**9**.

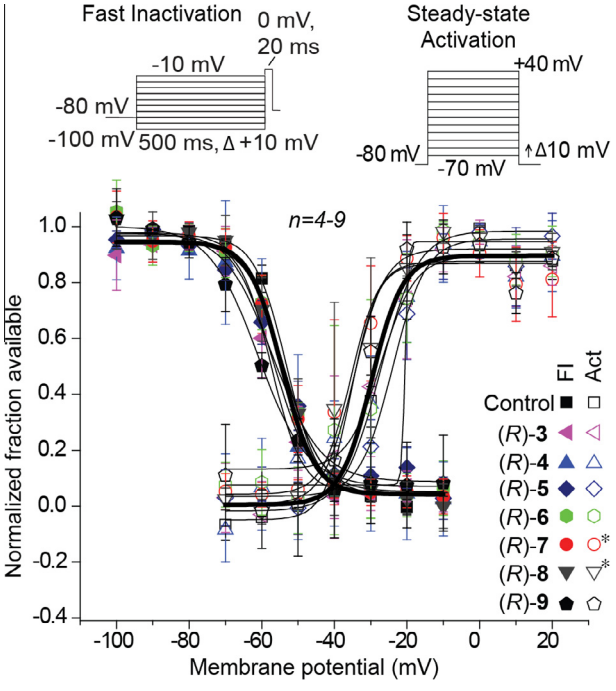

Figure 3. Effects of (*R*)-**3**–(*R*)-**9** on fast inactivation and steady-state activation states of Na^+ currents in embryonic cortical neurons. Voltage protocol for fast inactivation (*top left*) and activation (*top right*). Representative Boltzmann fits for steady-state fast inactivation and activation for cortical neurons treated with 0.1% DMSO (control, bolded curves) and the indicated compounds are shown. Values for $V_{1/2}$, the voltage of half-maximal inactivation and activation and the slope factors (k) were derived from Boltzmann distribution fits to the individual recordings and averaged to determine the mean (±SEM) voltage dependence of steady-state inactivation and activation, respectively. No significant differences were observed between control and fast inactivation or activation other than for (*R*)-**7** and (*R*)-**8** (*) for any of the conditions tested (p >0.05, one-way ANOVA). Data are from 5 to 7 cells per condition.

Finally, we tested if (*R*)-**3**–(*R*)-**9** could elicit frequency (use)-dependent blockage of Na^+ currents. The ability to block Na^+ currents in an activity- or use-dependent manner is a useful property for ASDs since it allows for preferential decreases in sodium channel availability during high- (i.e., seizures) but not low-frequency firing.[48] Thirty, identical test pulses were applied at 10 Hz (Fig. 4A).[9,39] The difference in available current was calculated by dividing the peak current at any given pulse ($pulse_N$) by the peak current in response to the initial pulse ($pulse_1$). Representative currents for this protocol are shown for control and 10 μM (*R*)-**7**-treated cells (Fig. 4B). None of the tested compounds exhibited statistically relevant frequency (use)-dependent inhibition of Na^+ currents (Fig. 4C).

The anticonvulsant activity for (*R*)-**9** led us to further explore the electrophysiological properties of this compound in CAD and HEK293 recombinant cells, which express a distinct population of Na_V channels.

2.3.2.2. CAD cells. CAD cells express endogenous tetrodotoxin-sensitive Na^+ currents that display rapid activation and inactivation kinetics upon membrane depolarization[39] and are likely composed mostly of $Na_V1.7$ channels with minor contributions by $Na_V1.1$, $Na_V1.3$, and $Na_V1.9$ channels.[9,42,49] We showed that the sodium channel properties of (*R*)-**1** in CAD cells[49] are similar to those in cultured neurons and in mouse N1E-115 neuroblastoma cells.[50] CAD cells were easily recorded from and cultured thus allowing us to conveniently determine (*R*)-**9** sodium channel slow inactivation, frequency (use)-dependence, steady-state activation, and fast inactivation properties over a range of concentrations. These properties were quantitatively compared with other (*R*)-**A** compounds, (*R*)-**1**, and (*S*)-**2**. Compound (*R*)-**9** promoted VGSC transition to a slow-inactivated state in a concentration-dependent manner; almost complete slow inactivation was observed at the highest concentration (Fig. 5A). To determine the comparative level to which (*R*)-**9** induced slow inactivation, we calculated concentration response curves for slow inactivation induction at −50 mV as well as at +20 mV; the IC_{50} inactivation values are shown in Figure 5A (boxes). Compared with our recently reported IC_{50} values of 85 and 13 μM for slow inactivation induced by (*R*)-**1**[9,20] and (*S*)-**2**,[10] the IC_{50} value for (*R*)-**9** (0.70 μM) was ~121-fold and ~19-fold lower, respectively, at −50 mV. Similar differences in the IC_{50} values were measured at +20 mV. Next, we tested for the effects of (*R*)-**9** on fast inactivation. We used a protocol tailored to induce a fast-inactivated state, as previously described.[9,10,20] Cells were subjected to prepulse potentials ranging from −120 to −10 mV in 10 mV increments for 500 ms. A 0 mV test pulse for 20 ms measures the available current. The 500 ms conditioning pulse allows for examination of the linear range of fast inactivation curves for endogenous channels at assayed potentials. As illustrated in Figure 5B, steady-state, fast inactivation curves of Na^+ currents from control (0.1% DMSO) and CAD neurons treated with various concentrations of (*R*)-**9** were well fitted with a single Boltzmann function (R^2 >0.979 for all conditions). The $V_{1/2}$ value for inactivation for 0.1% DMSO (control)-treated cells was −69.1 ± 3.6 mV (n = 7), which was significantly different from that of (*R*)-**9** (10 μM)-treated cells (−84.6 ± 1.6 mV; n = 6; $p<0.05$; Student's t-test; Fig. 5B). Because changes in Na^+ current amplitudes could be due to alterations in channel gating,[51] we tested if (*R*)-**9** altered the voltage-dependent activation properties of Na^+ currents. Activation changes for CAD cells treated with (*R*)-**9** were measured by whole-cell ionic conductances in response to changes in command voltage and analyzed by comparing Boltzmann properties of midpoints ($V_{1/2}$) and slope factors (k). We found that VGSC steady-state activation properties were no different between 0.1% DMSO (control; $V_{1/2}$ for activation = −19.5 ± 2.8 mV (n = 8)) and any concentration tested for (*R*)-**9** (Fig. 5B). Finally, we tested if (*R*)-**9** could confer frequency (use)-dependent Na^+ current block. Thirty, identical test pulses were applied at 10 Hz as described previously.[9,10,20] The available current in control cells (0.1% DMSO) and treated cells (various concentrations of (*R*)-**9**) was calculated by dividing the peak current at any given pulse ($pulse_N$) by the peak current in response to the initial pulse ($pulse_1$). Compound (*R*)-**9** exhibited frequency (use)-dependent inhibition of Na^+ currents (Fig. 5C), and by the last pulse, compared with control (0.1% DMSO), the peak current was ~39% lower in the presence of 10 μM (*R*)-**9**. When we tested 30 μM (*R*)-**10** in a similar protocol, we observed ~44% inhibition in Na^+ currents (data not shown).

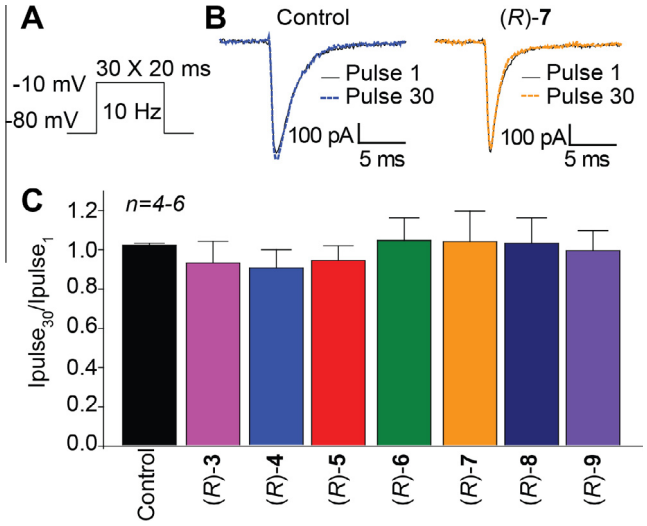

Figure 4. Effects of (*R*)-**3**–(*R*)-**9** on frequency (use)-dependent block of Na^+ currents in embryonic cortical neurons. (A) The frequency (use)-dependence of block was examined by holding cells at the hyperpolarized potential of −80 mV and evoking currents at 10 Hz by 20 ms test pulses to −10 mV. (B) Representative overlaid traces are illustrated by pulses 1 and 30 for control (0.1% DMSO) and in the presence of (*R*)-**7** (10 μM). C. Summary of the maximal decrement in current amplitude observed at the end of the 30-pulse train for control or 10 μM of the indicated compounds. None of the compounds exhibited any degree of frequency (use)-dependence (p >0.05, one-way ANOVA with Dunnett's post-hoc test). Data are from 4 to 6 cells per condition.

2.3.2.3. HEK293 recombinant cells. In order to test if (*R*)-**9** had effects on various sodium channel isoforms, we examined the effects of 10 μM (*R*)-**9** on slow inactivation, fast inactivation, steady-state activation, and frequency (use)-dependence in HEK293 cells that stably expressed CNS ($hNa_V1.1$, $rNa_V1.3$), peripheral nervous system ($hNa_V1.7$), and cardiac ($hNa_V1.5$) channels using voltage protocols[9] illustrated in Figure 6A and K. The results of these experiments are summarized in Table 2. Notably, (*R*)-**9** exhibited similar, though not identical, effects on these biophysical properties irrespective of sodium channels, indicating that this compound exhibited little isoform specificity. We observed that (*R*)-**9** robustly transitioned the four sodium channel subtypes to the slow-inactivated state; that (*R*)-**9** shifted the $V_{1/2}$ of fast inactivation for $Na_V1.7$ by ~20.2 mV in the hyperpolarizing direction without affecting $V_{1/2}$ values for any of the other channel isoforms; and that (*R*)-**9** had no effect on steady-state activation or on frequency (use)-inhibition of Na^+ currents carried by any of the $Na_V1.x$ channels.

2.3.3. Additional studies

Among the (*R*)-**D** compounds, (*R*)-**9** exhibited the most attractive anticonvulsant profile and potently inhibited sodium channel function. Accordingly, we conducted additional tests on this

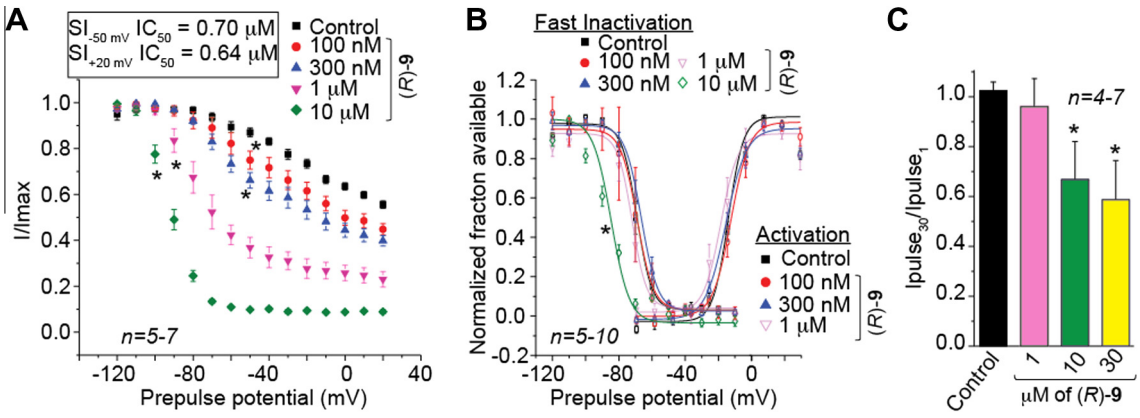

Figure 5. Effects of (*R*)-**9** on electrophysiological properties of Na^+ currents in CAD cells. (A) Summary of steady-state slow activation curves for CAD cells treated with 0.1% DMSO (control) or the indicated concentrations of (*R*)-**9**. Significant (*R*)-**9**-induced slow inactivation was evident; the starting voltages at which the extent of slow inactivation was significantly different from control are indicated by asterisks (*p <0.05, Student's t-test versus control). (B) Representative Boltzmann fits for steady-state fast inactivation and activation for CAD cells treated with 0.1% DMSO (control) and various concentrations of (*R*)-**9** are shown. Values for $V_{1/2}$, the voltage of half-maximal inactivation and activation and the slope factors (k) were derived from Boltzmann distribution fits to the individual recordings and averaged to determine the mean (±SEM) voltage dependence of steady-state inactivation and activation, respectively. Statistically significant differences between control and fast inactivation for 10 μM (*R*)-**9** are indicated by the asterisk (*p <0.05, one-way ANOVA). (C) Summary of the maximal decrement in current amplitude observed at the end of the 30-pulse train for control or 1, 10, or 30 μM of (*R*)-**9**. The two highest concentrations of (*R*)-**9** induced significant frequency (use)-dependence compared to control (p >0.05, one-way ANOVA with Dunnett's post-hoc test). Data are from 4 to 10 cells per condition as indicated.

chimeric compound. The observed anticonvulsant activity for (*R*)-**9** was further supported by its activities in the psychomotor 6 Hz test (44 mA) for therapy-resistant limbic seizures[19] (mouse, ip; ED_{50} = 44 mg/kg at 0.5 h), the corneal kindled seizure model[52] (mouse, ip; ED_{50} = 41 mg/kg at 0.25 h), and the rat hippocampal kindled seizure test for partial complex seizures or temporal lobe seizures[53,54] (rat, ip; ED_{50} = 22 mg/kg). Significantly, the 6 Hz (44 mA) test is a model for pharmacoresistant seizures,[19,55] and the mouse corneal kindling and the rat hippocampal tests are considered to be predicative models for partial-onset and partial complex seizures.[52]

Next, we evaluated (*R*)-**9** (10 μM) against a panel of seven human CYP450 enzymes and observed little or no direct inhibition for CYP1A2, CYP2B6, CYP2C8, CYP2C9, CYP2C19, CYP2D6 and CYP3A4/5 (data not shown). We found little or no time-dependent inhibition of these enzymes other than for CYP2C8 by (*R*)-**9**, for which there was an ~16% inhibition increase after a 30-min preincubation period. We also determined the pharmacokinetic properties for (*R*)-**9** in Sprague-Dawley rats (iv, po). Using a single iv dose of 5 mg/kg and an oral dose of 20 mg/kg, (*R*)-**9** showed excellent bioavailability (92%) and where the $t_{1/2}$ (iv) value was 1.75 h, the $t_{1/2}$ (po) value was 4.63 h, and the brain/plasma ratio was 1.2:1 at 6.0 h.

Compound (*R*)-**9** was evaluated at UNC's NIMH Psychoactive Drug Screening Program (PDSP)[56] against a battery of 43 receptors known to adversely impact drug effectiveness. No significant binding was observed at 10 μM. Moreover, (*R*)-**9** did not affect hERG K^+ channel activity (PatchExpress) at 30 μM (data not shown). Finally, we conducted a non-GLP 7-day repeated dose toxicity study for (*R*)-**9** in Sprague-Dawley female rats upon oral (gavage) administration at 20, 60, and 180 mg/kg/day dose levels. The no observed adverse effect level (NOAEL) for (*R*)-**9** was 60 mg/kg/day, providing a NOAEL/MES ED_{50} value of ~10. At higher dose levels, effects were observed in the ability to bear weight, coordination in gait, respiratory rate, relative organ weight (e.g., increase in liver, decrease in spleen and thymus), clinical chemistry parameters, and gross pathology (data not shown).

3. Discussion

Many of the (*R*)-**D** chimeric compounds exhibited excellent anticonvulsant activities in the MES model (mice, ip), comparable with the parent compounds (*R*)-**1**[11,30] and (*S*)-**2**[15] (ED_{50} (mg/kg): (*R*)-**3**, >10, <30; (*R*)-**4**, 5.5; (*R*)-**5**, 9.4; (*R*)-**6**, 14; (*R*)-**7**, ~10; (*R*)-**8**, 13; (*R*)-**9**, 6.5; (R)-**1**, 4.5; (*S*)-**2**, 4.1). Furthermore, we observed only modest differences in seizure protection when the X-substituent in (*R*)-**D** was varied from electron-withdrawing to electron-donating. Earlier studies on (*R*)-**A** compounds where the linker (L) was either a single bond[9] ((*R*)-**E**) or an oxymethylene group[10] ((*R*)-**F**) showed that the electron-withdrawing, trifluoromethoxy (OCF_3) group provided the greatest protection in the seizure models. For (*R*)-**D**, we found the most active compounds to be the 3″-F ((*R*)-**4**) and the 3″-OCF_3 ((*R*)-**9**) derivatives (MES ED_{50} (mice, ip, mg/kg): (*R*)-**4**, 5.5; (*R*)-**9**, 6.5; MES ED_{50} (rat, po, mg/kg): (*R*)-**4**, <10; (*R*)-**9**, 8.3); however, the differences in their activities from the other compounds in the series were not great.

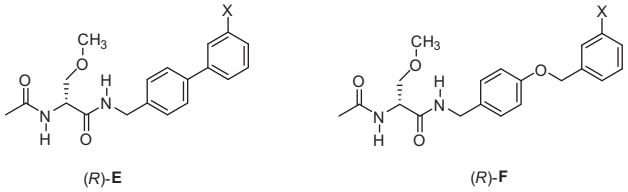

For the (*R*)-**E** and (*R*)-**F** chimeric compounds, we determined their slow inactivation IC_{50} values in CAD cells.[9,10] Accordingly, we measured the IC_{50} value for (*R*)-**9** in CAD cells to gauge the relative potency of this series with the two earlier sets of compounds. We found the (R)-**9** slow inactivation IC_{50} (−50 mV) value to be 0.70 μM (Fig. 5), which is comparable to the values for the corresponding (*R*)-**E** and (*R*)-**F** derivatives, (*R*)-**40** and (*R*)-**41**, respectively (IC_{50} (μM): (*R*)-**9**, 0.70; (*R*)-**40**, 0.85;[9] (*R*)-**41**, 0.24[10]). Similarly, we found that (*R*)-**9** in CAD cells, like (*R*)-**40**[9] and (*R*)-**41**,[10] inhibited Na^+ currents in a frequency (use)-dependent manner, but unlike these two, we observed that (*R*)-**9** affected fast inactivation at the highest concentration (10 μM) tested (Fig. 5).

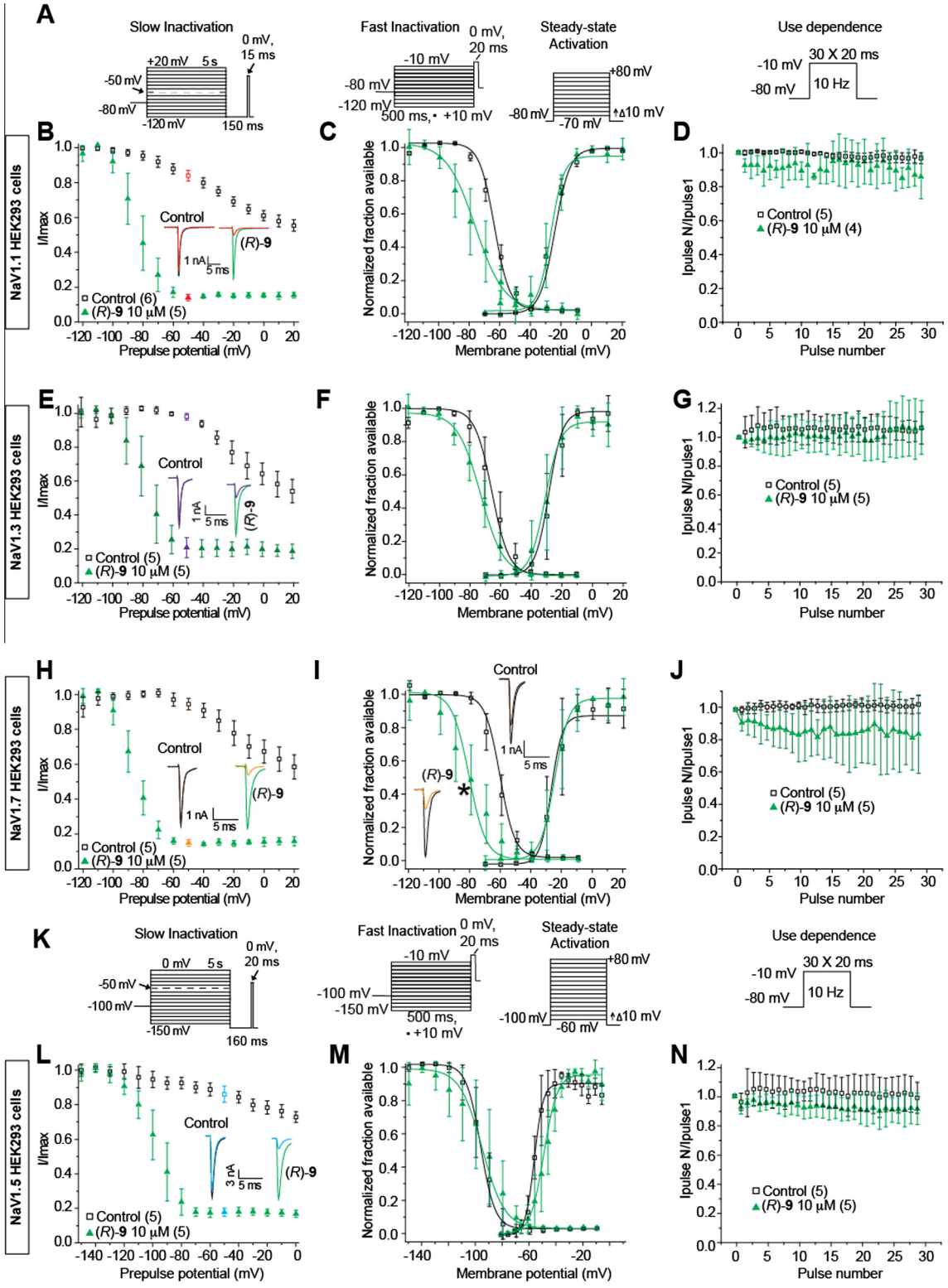

Figure 6. Analysis of (*R*)-**9** on electrophysiological properties of $Na_V1.1$, $Na_V1.3$, $Na_V1.7$, and $Na_V1.5$ currents in HEK293 cells. (A and K) Voltage protocols for examining slow inactivation, fast inactivation, steady-state activation and frequency (use)-dependent block. $Na_V1.5$ uses hyperpolarized protocols due to differences in the hyperpolarized activation typical for this isoform. (B, E, H and L) Summary of steady-state slow activation curves for HEK293 cells treated with 0.1% DMSO (control) or 10 μM (*R*)-**9**. Insets illustrate representative current traces from HEK293 cells in the absence (control, 0.1% DMSO) or presence of 10 μM (*R*)-**9**. Traces represent the currents evoked at −120 (black or green) and −50 mV (red, purple, orange, or cyan). (C, F, I and M) Representative Boltzmann fits for steady-state fast inactivation and activation for HEK293 cells treated with 0.1% DMSO (control) or 10 μM of (*R*)-**9**. Values for $V_{1/2}$, the voltage of half-maximal inactivation and activation, and the slope factors (k) were derived from Boltzmann distribution fits to the individual recordings and were averaged to determine the mean (±SEM) voltage dependence of steady-state inactivation and activation, respectively. (*R*)-**9** significantly shifted the $V_{1/2}$ of fast inactivation for $Na_V1.7$ by ~20.2 mV in the hyperpolarizing direction (*p <0.05, Student's t-test versus control) while the $V_{1/2}$s for $Na_V1.1$, $Na_V1.3$, and $Na_V1.5$ were not affected. (D, G, J and N) Summary of average frequency (use)-dependent decrease in current amplitude over time (±SEM) produced by control (0.1% DMSO) or 10 μM (*R*)-**9**. Data are from 5 to 6 cells per condition.

Please cite this article in press as: Torregrosa, R.; et al. *Bioorg. Med. Chem.* (2015), http://dx.doi.org/10.1016/j.bmc.2015.04.014

Table 2
Comparative current densities, cell capacitances, and Boltzmann parameters of voltage-dependence of channel activation and steady-state fast inactivation curves for control- and (*R*)-*N*-4′-((3″-trifluoromethoxy)phenoxy)benzyl 2-acetamido-3-methoxypropionamide ((*R*)-**9**)-treated HEK293 cells expressing $Na_V1.1$, $Na_V1.3$, $Na_V1.7$ or $Na_V1.5$ channels

Condition	Extent of slow inactivation (at −50 mV)[a]	Voltage-dependence of activation[b]		Voltage-dependence of fast inactivation		Use-dependent inhibition[c]
		$V_{1/2}$ (mV)	Slope (mV/e-fold)	$V_{1/2}$ (mV)	Slope (mV/e-fold)	
$Na_V1.1$						
Control	0.19 ± 0.04 (5)	−24.69 ± 1.52 (5)	4.22 ± 0.60 (5)	−64.11 ± 3.63 (6)	5.93 ± 1.48 (6)	0.98 ± 0.02 (5)
10 μM (*R*)-**9**	0.87 ± 0.04 (6)*	−24.43 ± 2.94 (6)	4.64 ± 1.78 (5)	−76.72 ± 4.11 (5)	6.89 ± 2.11 (6)	0.85 ± 0.17 (6)
$Na_V1.3$						
Control	0.04 ± 0.02 (5)	−29.62 ± 3.59 (5)	4.17 ± 1.97 (5)	−65.44 ± 5.62 (5)	5.51 ± 1.12 (5)	1.12 ± 0.19 (5)
10 μM (*R*)-**9**	0.78 ± 0.04 (5)*	−32.48 ± 5.48 (4)	4.47 ± 1.46 (4)	−72.84 ± 4.11 (5)	7.19 ± 2.19 (5)	1.23 ± 0.18 (5)
$Na_V1.7$						
Control	0.06 ± 0.03 (5)	−27.13 ± 4.01 (5)	3.81 ± 1.24 (5)	−61.11 ± 3.02 (5)	5.13 ± 1.22 (5)	1.03 ± 0.09 (5)
10 μM (*R*)-**9**	0.87 ± 0.04 (5)*	−24.98 ± 4.22 (5)	4.01 ± 1.43 (5)	−81.35 ± 6.70 (5)*	5.52 ± 1.68 (5)	0.82 ± 0.22 (5)
$Na_V1.5$						
Control	0.07 ± 0.03 (5)	−55.71 ± 3.81 (5)	3.26 ± 1.75 (5)	−96.54 ± 1.64 (5)	5.34 ± 0.86 (4)	1.05 ± 0.15 (5)
10 μM (*R*)-**9**	0.81 ± 0.04 (5)*	−48.99 ± 4.79 (5)	3.39 ± 1.69 (7)	−95.36 ± 2.43 (5)	6.12 ± 0.72 (7)	0.92 ± 0.14 (5)

[a] The extent of slow inactivation was calculated as 1 minus the normalized peak I_{Na} and denotes the fraction of channels that have transitioned to a non-conducting (slow-inactivated) state at −50 mV.
[b] Values for $V_{1/2}$, the voltage of half-maximal activation, and slope, were derived from Boltzmann distribution fits to the individual recordings and averaged to determine the mean and standard error of the mean (±SEM).
[c] Fraction of current remaining at the end of the 30-pulse train, normalized to the first pulse. *N* values are indicated in parentheses. The protocols used for these parameters are illustrated in Figure 6. Asterisks represent statistically significant differences as compared to control within each tested group (p <0.05, Student's t-test).

These overall results suggest that the composition and size of the different linkers in (*R*)-**D**–(*R*)-**F** did not appreciably affect the interaction of the chimeric compounds with the VGSCs.

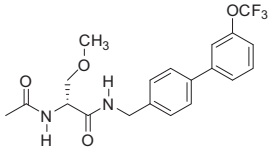

(*R*)-**40**

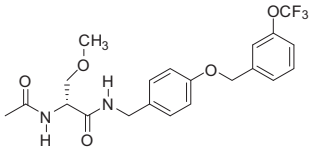

(*R*)-**41**

Our finding that (*R*)-**9** promoted sodium channel slow inactivation in rat embryonic cortical neurons that express $Na_V1.1$, $Na_V1.2$, $Na_V1.3$, and $Na_V1.6$ channels[36] and in CAD cells that largely express $Na_V1.7$ channels[9,42,49] suggested that this compound showed little Na_V channel subtype selectivity. We explored this by testing (*R*)-**9** in HEK293 recombinant cells[9] that expressed $hNa_V1.1$, $rNa_V1.3$, $hNa_V1.5$, or $hNa_V1.7$ (Fig. 6). In agreement with this notion, (*R*)-**9** (10 μM) potently transitioned the sodium channels to the slow-inactivated state regardless of the Na_V channel isoform. In the recombinant cells, we observed that the effect of (*R*)-**9** was different on sodium channel fast inactivation and frequency (use)-dependent inhibition. A similar result was previously reported for a (*R*)-**E** compound where X = Cl.[9]

The anticonvulsant activities for the (*R*)-**D** compounds are attributed, in part, to their ability to modulate VGSC activities. Using rat embryonic cortical neurons that express $Na_V1.1$, $Na_V1.2$, $Na_V1.3$, and $Na_V1.6$ channels,[40] we learned that the (*R*)-**D** compounds uniformly promoted slow inactivation (Fig. 2). At 10 μM, the 3″-unsubstituted derivative (*R*)-**3** was the most potent, followed by the 3″-electron-withdrawing derivatives (*R*)-**4**, (*R*)-**5**, (*R*)-**9**, (*R*)-**7**, and then the two 3″-electron-donating derivatives (*R*)-**6** and (*R*)-**8** (Fig. 2C). Interestingly, the relative level of slow inactivation for the (R)-**D** compounds did not parallel their corresponding anticonvulsant activities. For example, (*R*)-**3** showed the greatest level of slow inactivation (Fig. 2C), but it was the least potent in the MES seizure model in mice (ip) (Table 1). When we compared the slow inactivation IC_{50} (−50 mV) values for (*R*)-**9** and (*R*)-**1** in CAD cells, we found that the IC_{50} value for (*R*)-**9** was 0.70 μM, which was ~120-fold lower than the value reported for (*R*)-**1** (85 μM). Despite (*R*)-**9**'s increased potency, we did not find a comparable increased protection for (*R*)-**9** versus (*R*)-**1** in the MES seizure model in mice (ip) (ED_{50} (mg/kg): (*R*)-**9**, 6.5; (*R*)-**1**, 4.5). A similar lack of correspondence for the CAD slow inactivation IC_{50} values and their in vivo seizure protection activities in the MES test (mice, ip) were observed for the (*R*)-**E** and the (*R*)-**F** compounds with (*R*)-**1** (CAD cells slow inactivation IC_{50} (−50 mV, μM): (*R*)-**40**, 0.85; (*R*)-**41**, 0.24; (*R*)-**1**, 85; ED_{50} (mg/kg): (*R*)-**40**, 4.7; (*R*)-**41**, 12; (*R*)-**1**, 4.5).[9,10] We tentatively attribute this finding to the multiple factors that contribute to whole animal pharmacological activity, the sodium channel composition in CAD cells versus those in the CNS, the possibility that additional, unidentified pathways exist for seizure control, and the recognition that patch-clamp electrophysiology studies do not recapitulate conditions created in the seizure models.

4. Conclusion

Many of the chimeric (*R*)-**D** compounds displayed potent anticonvulsant activities and high PI values, which were similar to ASDs, in the MES test when administered to rodents. The chimeric compounds' anticonvulsant activities likely stemmed, at least in part, from their ability to promote sodium channel slow inactivation. VGSCs are responsible for the initiation of and the sustained activity of neuronal signaling during seizure events. The well described mechanism of action for both (*R*)-**D** parent compounds, lacosamide and safinamide, involve inhibition of these channels.[14,15,37,38] Phenytoin, lamotrigine, and carbamazepine are among other ASDs that have primary activity on VGSCs to restrict neuronal firing during seizures.[57] As evident by perturbation of VGSC slow inactivation (Fig. 2), the class (*R*)-**D** compounds potently shifted VGSC availability, which readily explains anticonvulsant activity. The type of channel block produced by these compounds is also a desirable characteristic for ASDs. By selectively affecting sodium channel slow inactivation or frequency (use)-dependent block, these compounds can promote channel inhibition in response to sustained use (i.e., epileptic activity).

5. Experimental

5.1. General methods

Melting points were determined in open capillary tubes using a Thomas–Hoover melting point apparatus and are uncorrected.

Optical rotations were obtained on a Jasco P-1030 polarimeter at the sodium D line (589 nm) using a 1 dm path length cell. NMR spectra were obtained at 400 MHz (^{1}H) and 100 MHz (^{13}C) using TMS as an internal standard. Chemical shifts (δ) are reported in parts per million (ppm) from tetramethylsilane. Low-resolution mass spectra were obtained with a BioToF-II-Bruker Daltonics spectrometer by Dr. S. Habibi at the University of North Carolina Department of Chemistry. The high-resolution mass spectrum was performed on a Bruker Apex-Q 12 Telsa FTICR spectrometer by Dr. S. Habibi. Microanalyses were performed by Atlantic Microlab, Inc. (Norcross, GA). Reactions were monitored by analytical thin-layer chromatography (TLC) plates (Aldrich, Cat # Z12272-6) and analyzed with 254 nm UV light. The reactions were purified by flash column chromatography using silica gel (Dynamic Adsorbents Inc., Cat # 02826-25). All chemicals and solvents were reagent grade and used as obtained from commercial sources without further purification. Yields reported are for purified products and were not optimized. Compounds were checked by TLC, ^{1}H and ^{13}C NMR, MS, and elemental analyses. The analytical results are within ±0.40% of the theoretical value. The TLC, NMR and the analytical data confirmed the purity of the products was ⩾95%.

5.1.1. General procedure for the deprotection and acetylation of (*R*)-*N*-benzyl 2-*N*-(*tert*-butoxycarbonyl)amino-3-methoxypropionamide derivatives (*R*)-34–(*R*)-39 to give (*R*)-3 and (*R*)-5–(*R*)-9 (Method 1)

A CH_2Cl_2 solution (0.1–0.3 M) of the *tert*-butoxycarbonyl-compound ((*R*)-**34**–(*R*)-**39**) was treated with 4 M HCl in dioxane (3–4 equiv) at room temperature (2–12 h). The reaction mixture was evaporated in vacuo. The resulting residue was dissolved in CH_2Cl_2 (0.1–0.3 M) and then triethylamine (2–3 equiv) and acetyl chloride (1.0–1.2 equiv) were carefully added at 0 °C and the resulting solution was stirred at room temperature (2–16 h). The solution was washed with an aqueous 10% citric acid solution followed by a saturated aqueous $NaHCO_3$ solution. The organic layer was dried (Na_2SO_4) and concentrated in vacuo. The residue was purified by column chromatography on SiO_2 and/or recrystallized with EtOAc/hexanes.

5.1.2. (*R*)-*N*-4′-Phenoxybenzyl 2-*N*-Acetamido-3-methoxypropionamide ((*R*)-3)

Using Method 1, (*R*)-**34** (1.27 g, 3.17 mmol), 4 M HCl (5.6 mL), Et_3N (962 mg, 9.51 mmol), and AcCl (298 mg, 3.80 mmol) gave the desired compound (*R*)-**3** as a white solid (981 mg, 90%): R_f = 0.27 (20:1 CH_2Cl_2/MeOH); mp 147–148 °C; $[\alpha]_D^{24}$ −16.1° (*c* 1.0, $CHCl_3$); ^{1}H NMR ($CDCl_3$) δ 2.03 (s, C*H*$_3$C(O)), 3.39 (s, OC*H*$_3$), 3.46 (dd, *J* = 4.3, 9.3 Hz, C*H*H′OCH$_3$), 3.81 (dd, *J* = 4.3, 9.3 Hz, CH*H*′OCH$_3$), 4.40–4.48 (m, NHC*H*$_2$), 4.58 (dt, *J* = 4.3, 7.0 Hz, C*H*CH$_2$), 6.49 (d, *J* = 7.0 Hz, N*H*), 6.83–6.93 (m, 2Ar*H*, N*H*), 6.93–6.97 (m, Ar*H*), 7.00 (d, *J* = 8.2 Hz, 2Ar*H*), 7.27 (d, *J* = 8.2 Hz, 2Ar*H*), 7.32 (m, 2Ar*H*), addition of excess (*R*)-(−)-mandelic acid to a $CDCl_3$ solution of (*R*)-**3** gave only one signal for the acetyl methyl and one signal for the methoxy protons; ^{13}C NMR ($CDCl_3$) δ 23.2 (C(O)**C**H$_3$), 43.0 (NH**C**H$_2$), 52.4 (**C**HCH$_2$), 59.1 (O**C**H$_3$), 71.6 (CH**C**H$_2$), 118.9, 119.0, 123.3, 128.9, 132.7, 156.7 (Ar**C**), 169.9, 170.3 (2 **C**(O)), the remaining two aromatic peaks were not detected and are believed to overlap with nearby signals; LRMS (ESI$^+$) 365.1 [M+Na]$^+$ (calcd for $C_{19}H_{22}N_2O_4Na^+$ 365.1); HRMS (ESI$^+$) 365.1478 [M+Na]$^+$ (calcd for $C_{19}H_{22}N_2O_4Na^+$ 365.1478); Anal. Calcd for $C_{19}H_{22}N_2O_4$: C, 66.65; H, 6.48; N, 8.18. Found: C, 66.41; H, 6.36; N, 8.14.

5.1.3. (*R*)-*N*-4′-((3″-Chloro)phenoxy)benzyl 2-*N*-Acetamido-3-methoxypropionamide ((*R*)-5)

Using Method 1, (*R*)-**35** (1.30 g, 2.99 mmol), 4 M HCl (4.5 mL), Et_3N (908 mg, 8.97 mmol), and AcCl (282 mg, 3.59 mmol) gave the desired compound (*R*)-**5** as a white solid (786 mg, 70%): R_f = 0.29 (20:1 CH_2Cl_2/MeOH); mp 129–130 °C; $[\alpha]_D^{24}$ −19.9° (*c* 1.0, $CHCl_3$); ^{1}H NMR ($CDCl_3$) δ 2.04 (s, C*H*$_3$C(O)), 3.39 (s, OC*H*$_3$), 3.41–3.49 (m, C*H*H′OCH$_3$), 3.75–3.86 (m, CH*H*′OCH$_3$), 4.41–4.52 (m, NHC*H*$_2$), 4.52–4.60 (m, C*H*CH$_2$), 6.46 (d, *J* = 7.0 Hz, N*H*), 6.76–6.85 (m, Ar*H*), 6.85–6.91 (m, N*H*), 6.94–7.03 (m, 3Ar*H*), 7.05–7.15 (m, Ar*H*), 7.20–7.26 (m, 2Ar*H*), 7.30–7.37 (m, Ar*H*), addition of excess (*R*)-(−)-mandelic acid to a $CDCl_3$ solution of (*R*)-**5** gave only one signal for the acetyl methyl and one signal for the methoxy protons; ^{13}C NMR ($CDCl_3$) δ 23.1 (C(O)**C**H$_3$), 42.9 (NH**C**H$_2$), 52.5 (**C**HCH$_2$), 59.1 (O**C**H$_3$), 71.8 (CH**C**H$_2$), 116.6, 118.9, 119.5, 123.3, 129.0, 130.5, 132.7, 133.6, 155.6, 158.2 (Ar**C**), 170.0, 170.3 (**C**(O)); LRMS (ESI$^+$) 377.1 [M+H]$^+$ (calcd for $C_{19}H_{21}ClN_2O_4H^+$ 377.1); HRMS (ESI$^+$) 377.1269 [M+H]$^+$ (calcd for $C_{19}H_{21}ClN_2O_4H^+$ 377.1268); Anal. Calcd for $C_{19}H_{21}ClN_2O_4$: C, 60.56; H, 5.62; Cl, 9.41; N, 7.43. Found: C, 60.69; H, 5.60; Cl, 9.14; N, 7.32.

5.1.4. (*R*)-*N*-4′-((3″-Methyl)phenoxy)benzyl 2-*N*-acetamido-3-methoxypropionamide ((*R*)-6)

Using Method 1, (*R*)-**36** (2.10 g, 5.07 mmol), 4 M HCl (7.6 mL), Et_3N (1.54 g, 15.2 mmol), and AcCl (447 mg, 6.08 mmol) gave the desired compound (*R*)-**6** as a white solid (1.25 g, 69%): R_f = 0.27 (20:1 CH_2Cl_2/MeOH); mp 110–111 °C; $[\alpha]_D^{24}$ −19.2° (*c* 1.0, $CHCl_3$); ^{1}H NMR ($CDCl_3$) δ 2.05 (s, C*H*$_3$C(O)), 2.34 (s, C*H*$_3$), 3.39 (s, OC*H*$_3$), 3.42–3.48 (m, C*H*H′OCH$_3$), 3.83 (dd, *J* = 4.3, 9.3 Hz, CH*H*′OCH$_3$), 4.40–4.52 (m, NHC*H*$_2$), 4.54–4.57 (m, C*H*CH$_2$), 6.42 (d, *J* = 7.0 Hz, N*H*), 6.68–6.77 (m, Ar*H*), 6.77–6.85 (m, Ar*H*, N*H*), 6.90–7.00 (m, 3Ar*H*), 7.18–7.26 (m, 3Ar*H*), addition of excess (*R*)-(−)-mandelic acid to a $CDCl_3$ solution of (*R*)-**6** gave only one signal for the acetyl methyl and one signal for the methoxy protons; ^{13}C NMR ($CDCl_3$) δ 21.3 (Ar**C**H$_3$), 23.1 (C(O)**C**H$_3$), 42.9 (NH**C**H$_2$), 52.4 (**C**HCH$_2$), 59.0 (O**C**H$_3$), 71.8 (CH**C**H$_2$), 115.9, 118.9, 119.5, 124.1, 128.8, 129.4, 132.5, 139.9, 156.7, 157.0 (Ar**C**), 169.9, 170.3 (**C**(O)); LRMS (ESI$^+$) 357.1 [M+H]$^+$ (calcd for $C_{20}H_{24}N_2O_4H^+$ 357.1); HRMS (ESI$^+$) 357.1814 [M+H]$^+$ (calcd for $C_{20}H_{24}N_2O_5H^+$ 357.1814); Anal. Calcd for $C_{20}H_{24}N_2O_4$: C, 67.40; H, 6.79; N, 7.86. Found: C, 67.34; H, 6.79; N, 7.85.

5.1.5. (*R*)-*N*-4′-((3″-Trifluoromethyl)phenoxy)benzyl 2-*N*-Acetamido-3-methoxypropionamide ((*R*)-7)

Using Method 1, (*R*)-**37** (1.65 g, 3.5 mmol), 4 M HCl (4.0 mL), Et_3N (1.07 mg, 10.6 mmol), AcCl (414 mg, 5.3 mmol) gave the desired compound (*R*)-**7** as a white solid (1.23 mg, 85%): R_f = 0.32 (20:1 CH_2Cl_2/MeOH); mp 115-117 °C; $[\alpha]_D^{24}$ −11.1° (*c* 1.0, $CHCl_3$); ^{1}H NMR ($CDCl_3$) δ 2.05 (s, C*H*$_3$C(O)), 3.39 (s, OC*H*$_3$), 3.45 (dd, *J* = 4.3, 9.1 Hz, C*H*H′OCH$_3$), 3.83 (dd, *J* = 4.3, 9.1 Hz, CH*H*′OCH$_3$), 4.41–4.52 (m, NHC*H*$_2$), 4.56 (dt, *J* = 4.3, 6.8 Hz, C*H*CH$_2$), 6.38–6.50 (m, N*H*), 6.73–6.85 (m, N*H*), 6.95–7.04 (m, 2Ar*H*), 7.06–7.18 (m, 2Ar*H*), 7.21–7.26 (m, Ar*H*), 7.29 (s, Ar*H*), 7.32–7.48 (m, 2Ar*H*), addition of excess (*R*)-(−)-mandelic acid to a $CDCl_3$ solution of (*R*)-**7** gave only one signal for the acetyl methyl and one signal for the methoxy protons; ^{13}C NMR ($CDCl_3$) δ 23.2 (C(O)**C**H$_3$), 42.9 (NH**C**H$_2$), 52.4 (**C**HCH$_2$), 59.1 (O**C**H$_3$), 71.6 (CH**C**H$_2$), 110.0 (Ar**C**), 115.2 (q, *J* = 4.0 Hz, Ar**C**), 119.5, 119.6 (Ar**C**), 120.2 (q, *J* = 4.0 Hz, Ar**C**), 120.7, 121.6, 129.1 (Ar**C**), 131.9 (q, *J* = 272.0 Hz, **C**F$_3$), 133.6 (q, *J* = 32.0 Hz, Ar**C**), 155.8 (Ar**C**), 170.0, 170.3 (**C**(O)); LRMS (ESI$^+$) 411.2 [M+H]$^+$ (calcd for $C_{20}H_{21}F_3N_2O_4H^+$ 411.2); HRMS (ESI$^+$) 411.1531 [M+H]$^+$ (calcd for $C_{20}H_{21}F_3N_2O_4H^+$ 411.1527); Anal. Calcd for $C_{20}H_{21}F_3N_2O_4{\cdot}0.15H_2O$: C, 58.53; H, 5.16; F, 13.89; N, 6.83. Found: C, 58.15; H, 5.20; F, 13.80; N, 6.78.

5.1.6. (*R*)-*N*-4′-((3″-Methoxy)phenoxy)benzyl 2-*N*-Acetamido-3-methoxypropionamide ((*R*)-8)

Using Method 1, (*R*)-**38** (1.00 g, 2.32 mmol), 4 M HCl (3.5 mL), Et_3N (704 mg, 6.96 mmol), and AcCl (218 mg, 2.78 mmol) gave the desired compound (*R*)-**8** as a white solid (742 mg, 86%):

R_f = 0.27 (20:1 CH_2Cl_2/MeOH); mp 123–124 °C; $[\alpha]_D^{24}$ −18.8° (*c* 1.0, $CHCl_3$); ^{1}H NMR ($CDCl_3$) δ 2.04 (s, $CH_3C(O)$), 3.39 (s, OCH_3), 3.45 (t, *J* = 9.3 Hz, $CHH'OCH_3$), 3.78 (s, OCH_3), 3.82 (dd, *J* = 4.3, 9.3 Hz, $CHH'OCH_3$), 4.39–4.51 (m, $NHCH_2$), 4.52–4.59 (m, $CHCH_2$), 6.45 (d, *J* = 7.0 Hz, N*H*), 6.54–6.60 (m, 2Ar*H*), 6.63–6.69 (m, Ar*H*), 6.78 (br s, N*H*), 6.95–7.01 (m, 2Ar*H*), 7.19–7.26 (m, 3Ar*H*), addition of excess (*R*)-(−)-mandelic acid to a $CDCl_3$ solution of (*R*)-**8** gave only one signal for the acetyl methyl and one signal for the methoxy protons; ^{13}C NMR ($CDCl_3$) δ 23.2 (C(O)**C**H_3), 43.0 ($NHCH_2$), 52.4 (**C**HCH_2), 55.3 (Ar**O**CH_3), 59.1 (**O**CH_3), 71.7 ($CHCH_2$), 104.9, 108.9, 110.9, 119.2, 128.9, 130.1, 132.8, 156.4, 158.3, 161.0 (Ar**C**), 169.9, 170.3 (**C**(O)); LRMS (ESI$^+$) 373.2 $[M+H]^+$ (calcd for $C_{20}H_{24}N_2O_5H^+$ 373.2); HRMS (ESI$^+$) 373.1764 $[M+H]^+$ (calcd for $C_{20}H_{24}N_2O_5H^+$ 373.1763); Anal. Calcd for $C_{20}H_{24}N_2O_5$: C, 64.50; H, 6.50; N, 7.52. Found: C, 64.51; H, 6.43; N, 7.42.

5.1.7. (*R*)-*N*-4′-((3″-Trifluoromethoxy)phenoxy)benzyl 2-*N*-Acetamido-3-methoxypropionamide ((*R*)-9)

Using Method 1, (*R*)-**39** (1.80 g, 3.72 mmol), 4 M HCl (6.0 mL), Et_3N (1.13 g, 11.2 mmol), AcCl (350 mg, 4.46 mmol) gave the desired compound (*R*)-**9** as a white solid (1.03 g, 65%): R_f = 0.27 (20:1 CH_2Cl_2/MeOH); mp 108–109 °C; $[\alpha]_D^{24}$ −15.1° (*c* 1.0, $CHCl_3$); ^{1}H NMR ($CDCl_3$) δ 2.04 (s, ($CH_3C(O)$), 3.39 (s, O**C**H_3), 3.45 (dd, *J* = 4.3, 9.3 Hz, $CHH'OCH_3$), 3.82 (dd, *J* = 4.1, 9.3 Hz, $CHH'OCH_3$), 4.39–4.51 (m, $NHCH_2$), 4.53–4.57 (m, $CHCH_2$), 6.43 (d, *J* = 7.0 Hz, N*H*), 6.70–6.80 (m, Ar*H*), 6.98 (d, *J* = 8.2 Hz, 2Ar*H*), 7.08–7.15 (m, Ar*H*), 7.23 (d, *J* = 8.2 Hz, 2Ar*H*), 7.30–7.38 (m, 2Ar*H*), addition of excess (*R*)-(−)-mandelic acid to a $CDCl_3$ solution of (*R*)-**9** gave only one signal for the acetyl methyl and one signal for the methoxy protons; ^{13}C NMR ($CDCl_3$) δ 23.2 (C(O)**C**H_3), 42.9 ($NHCH_2$), 52.5 (**C**HCH_2), 59.1 (O**C**H_3), 71.7 ($CHCH_2$), 111.3, 115.2, 116.4, 119.6 (Ar**C**), 120.3 (q, *J* = 257.0 Hz, **C**F_3), 129.1, 130.5, 133.8, 150.1, 155.5, 158.5 (Ar**C**), 170.0, 170.3 (**C**(O)); LRMS (ESI$^+$) 427.1 $[M+H]^+$ (calcd for $C_{20}H_{21}F_3N_2O_5H^+$ 427.1); HRMS (ESI$^+$) 427.1486 $[M+H]^+$ (calcd for $C_{20}H_{21}F_3N_2O_5H^+$ 427.1481).

5.2. Pharmacology

Compounds were screened under the auspices of the National Institutes of Health's ASP. Experiments were performed in male rodents (albino Carworth Farms No. 1 mice (ip), albino Sprague-Dawley rats (ip, po)). Housing, handling, and feeding were in accordance with recommendations contained in the *Guide for the Care and Use of Laboratory Animals*. Anticonvulsant activity was established using the MES test,[18] 6 Hz,[19] and the scMet test,[35] according to previously reported methods.[8,11]

5.3. Catecholamine A-differentiated (CAD) cells

CAD cells were grown at 37 °C and in 5% CO_2 (Sarstedt, Newton, NC) in Ham's F12/DMEM (GIBCO, Grand Island, NY), supplemented with 10% fetal bovine serum (Sigma, St. Louis, MO) and 1% penicillin/streptomycin (100% stocks, 10,000 U/mL penicillin G sodium and 10,000 μg/mL streptomycin sulfate).[49] Cells were passaged every 3–5 days at a 1:5 dilution.

5.4. Cortical neurons

Rat cortical neuron cultures were prepared from cortices dissected from embryonic day 19 cortices exactly as described.[58,59]

5.5. Culturing HEK293 cells expressing $Na_V1.1$, $Na_V1.3$, $Na_V1.5$, and $Na_V1.7$

$Na_V1.1$, $Na_V1.3$, $Na_V1.5$, and $Na_V1.7$ stable cells were grown under standard tissue culture conditions (5% CO_2 at 37 °C) in Dulbecco's modified Eagle's medium supplemented with 10% fetal bovine serum and 1% penicillin/streptomycin (100% stocks, 10,000 U/mL penicillin G sodium and 10,000 μg/mL streptomycin sulfate) as described before.[9]

5.6. Electrophysiology

Whole-cell voltage clamp recordings were performed at room temperature on cortical neurons, CAD cells, and HEK293 cells expressing $Na_V1.x$ isoforms using an EPC 10 Amplifier (HEKA Electronics, Lambrecht/Pfalz Germany) as described previously.[9,10,20] Electrodes were fabricated from standard-walled borosilicate glass capillaries (Warner Instruments, Hamden, CT) with a P-97 electrode puller (Sutter Instrument, Novato, CA) such that final electrode resistances were 1–2 MΩ when filled with internal solutions. The internal solution for recording Na^+ currents contained (in mM): 110 CsCl, 5 $MgSO_4$, 10 EGTA, 4 ATP Na_2-ATP, 25 HEPES (pH 7.2, 290–310 mOsm/L). The external solution contained (in mM): 100 NaCl, 10 tetraethylammonium chloride (TEA-Cl), 1 $CaCl_2$, 1 $CDCl_2$, 1 $MgCl_2$, 10 D-glucose, 4 4-AP, 0.1 $NiCl_2$, 10 HEPES (pH 7.3, 310–315 mOsm/L). Whole-cell capacitance and series resistance were compensated with the amplifier. Series resistance error was always compensated to be less than ±3 mV. Cells were considered for analysis only when the access resistance was less than 3 MΩ. Linear leak currents were digitally subtracted by -P/4 leak subtraction.

5.7. Data acquisition and analysis

Signals were filtered at 10 kHz and digitized at 10–20 kHz. Analysis was performed using Fitmaster and origin8.1 (OriginLab Corporation, MA, USA). For activation curves, conductance (*G*) through sodium channels was calculated using the equation $G = I/(V_m - V_{rev})$, where V_{rev} is the reversal potential, V_m is the membrane potential at which the current was recorded and *I* is the peak current. Activation and inactivation curves were fitted to a single-phase Boltzmann function $G/G_{max} = 1/\{1 + \exp[(V - V_{1/2})/k]\}$, where *G* is the peak conductance, G_{max} is the fitted maximal *G*, $V_{1/2}$ is the half-activation voltage, and *k* is the slope factor. Additional details of specific pulse protocols are described in the results text or figure legends.

5.8. Statistical analyses

Differences between means were compared by either paired or unpaired, two-tailed Student's *t*-tests or an analysis of variance (ANOVA), when comparing multiple groups (repeated measures whenever possible). If a significant difference was determined by ANOVA, then a Dunnett's or Tukey's post-hoc test was performed. Data are expressed as mean ± SEM, with $p < 0.05$ considered as the level of significance.

Acknowledgments

This work is supported by grants, in part, from the NINDS (1 R41 NS080278) and a National Scientist Development Award from the American Heart Association (SDG5280023 to R.K.). T.R.C. is supported by NIH Grant NS053422. We thank the NINDS and the ASP at the National Institutes of Health with Drs. Tracy Chen and John Kehne for kindly performing the pharmacological studies via the ASP's contract site at the University of Utah with Drs. H. Wolfe, H.S. White, and K. Wilcox. We express our appreciation to Dr. Bryan L. Roth and Mr. Jon Evans at the National Institute of Mental Health (NIMH) Psychoactive Drug Screening Project for performing in vitro receptor binding studies. This work was supported by NIMH Psychoactive Drug Screening Program, Contract

No. HHSN-271-2008-00025-C (NIMH-PDSP). The NIMH PDSP is directed by Bryan Roth MD, PhD at the University of North Carolina at Chapel Hill and Project Officer Jamie Driscol at NIMH, Bethesda MD, USA. The content is solely the responsibility of the authors and does not represent the official views of the National Center for Research Resources, National Institutes of Health. Harold Kohn has a royalty-stake position in (*R*)-**1** and is the founder of NeuroGate Therapeutics, Inc.

Supplementary data

Synthetic procedures, experimental and spectral data for the intermediates and final products evaluated in this study including tables for elemental analyses and high-resolution MS data; and ^{1}H NMR and ^{13}C NMR spectra for (*R*)-**3**, (*R*)-**5**–(*R*)-**9**. This material is available free of charge via the Internet.

Supplementary data associated with this article can be found, in the online version, at http://dx.doi.org/10.1016/j.bmc.2015.04.014.

References and notes

1. Centers for Disease Control and Prevention—Epilepsy. http://www.cdc.gov/epilepsy (accessed November 5, 2014).
2. McNamara, J. O. In *Goodman & Gilman The Pharmacological Basis of Therapeutics*; Brunton, L. L., Lazo, J. S., Parker, K. L., Eds., 11th ed.; McGraw-Hill: New York, NY, 2006; pp 501–525. Chapter 19.
3. Picot, M. C.; Baldy-Moulinier, M.; Daurs, J. P.; Dujols, P.; Crespel, A. *Epilepsia* **2008**, *49*, 1230.
4. Begley, C. E.; Lairson, D. R.; Reynolds, T. F.; Coan, S. *Epilepsy Res.* **2001**, *47*, 205.
5. Bauer, J.; Reuber, M. *Expert Opin. Emerg. Drugs* **2003**, *8*, 457.
6. Schmidt, D.; Rogawski, M. A. *Epilepsy Res.* **2007**, *50*, 71.
7. Loscher, W.; Brandt, C. *Pharmacol. Rev.* **2010**, *62*, 688.
8. Salome, C.; Salome-Grosjean, E.; Stables, J. P.; Kohn, H. *J. Med. Chem.* **2010**, *53*, 3756.
9. Lee, H.; Park, K. D.; Torregrosa, R.; Yang, X.-F.; Dustrude, E. T.; Wang, Y.; Wilson, S. M.; Barbosa, C.; Xiao, Y.; Cummins, T. R.; Khanna, R.; Kohn, H. *J. Med. Chem.* **2014**, *57*, 6165.
10. Park, K. D.; Yang, X.-F.; Dustrude, E. T.; Wang, Y.; Ripsch, M. S.; White, F. A.; Khanna, R.; Kohn, H. A. C. S. *Chem. Neurosci.* **2015**, *6*, 316.
11. Choi, D.; Stables, J. P.; Kohn, H. *J. Med. Chem.* **1996**, *39*, 1907.
12. Pavarello, P.; Bonsignori, A.; Dostert, P.; Heidempergher, F.; Pinciroli, V.; Colombo, M.; McArthur, R. A.; Salvati, P.; Post, C.; Fariello, R. G.; Varasi, M. *J. Med. Chem.* **1998**, *41*, 579.
13. Fariello, R. G. *Neurotherapeutics* **2007**, *4*, 110.
14. Perucca, E.; Yasothan, U.; Clincke, G.; Kirkpatrick, P. *Nat. Rev. Drug Disc.* **2008**, *7*, 973.
15. Fariello, R. G.; McArtur, R. A.; Bonsignori, A.; Cervini, M. A.; Maj, R.; Marrari, P.; Pevarello, P.; Wolf, H. H.; Woodhead, J. W.; White, H. S.; Varasi, M.; Salvati, P.; Post, C. *J. Pharmacol. Exp. Ther.* **1998**, *285*, 397.
16. Malek, N.; Grosset, D. G. *J. Exp. Pharmacol.* **2012**, *4*, 85.
17. Leonetti, F.; Capaldi, C.; Pisani, L.; Nicolotti, O.; Muncipinto, G.; Stefanachi, A.; Cellamare, S.; Caccia, C.; Carotti, A. *J. Med. Chem.* **2007**, *50*, 4909.
18. White, H. S.; Woodhead, J. H.; Franklin, M. R.; Swinyard, E. A.; Wolf, H. H. In *Antiepileptic Drugs*; Levy, R. H., Mattson, R. H., Meldrum, B. S., Eds.; ; Raven Press: New York, NY, 1995; Vol. 1, pp 99–110. 4th ed..
19. Barton, M. E.; Klein, B. D.; Wolff, H. H.; White, H. S. *Epilepsy Res.* **2001**, *47*, 217.
20. Wang, Y.; Wilson, S. M.; Brittain, J. M.; Ripsch, M. S.; Salome, C.; Park, K. D.; White, A. W.; Khanna, R.; Kohn, H. *ACS Chem. Neurosci.* **2011**, *2*, 317.
21. Kuo, C.-C.; Bean, B. P. *Mol. Pharmacol.* **1994**, *46*, 716.
22. Kahlig, K. K.; Hirakawa, R.; Liu, L.; George, A. L., Jr.; Belardinelli, L.; Rajamani, S. *Mol. Pharmacol.* **2014**, *85*, 162.
23. Anderson, G. W.; Zimmerman, J. E.; Callahan, F. M. *J. Am. Chem. Soc.* **1967**, *87*, 5012.
24. Verkade, J. G.; Urgaonkar, S. *Org. Lett.* **2005**, *7*, 3319.
25. Chen, J.; Wang, X.; Zheng, X.; Ding, J.; Liu, M.; Wu, H. *Tetrahedron* **2012**, *68*, 8905.
26. Li, F.; Wang, Q.; Ding, Z.; Tao, F. *Org. Lett.* **2003**, *12*, 2169.
27. Sawyer, J. S.; Schmittling, E. A.; Palkowitz, J. A.; Smith, W. J., III *J. Org. Chem.* **1998**, *63*, 6338.
28. Weisman, G. R. In *Asymmetric Synthesis-Analytical Methods*; Morrison, J. D., Ed.; Academic Press: New York, NY, 1983; Vol. 1, pp 153–172. Chapter 8.
29. Stables, J. P.; Kupferberg, H. J. In *Molecular and Cellular Targets for Antiepileptic Drugs*; Avanzini, G., Tanganelli, P., Avoli, M., Eds.; John Libbey: London, 1977; pp 191–198.
30. Stoehr, T.; Kupferberg, H. J.; Stables, J. P.; Choi, D.; Harris, R. H.; Kohn, H.; Walton, N.; White, H. S. *Epilepsy Res.*. **2007**, *74*, 147.
31. Porter, R. J.; Cereghino, J. J.; Gladding, G. D.; Hessie, B. J.; Kupferberg, H. J.; Scoville, B.; White, B. G. *Cleve. Clin. Q.* **1984**, *51*, 293.
32. Public Access to Neuroactive & Anticonvulsant Chemical Evaluations (PANAChE) Database. http://panache@nins.nih.gov (accessed November 5, 2014).
33. Dunham, N. W.; Miya, T.-S. *J. Am. Pharm. Assoc.* **1957**, *46*, 208.
34. White, H. S.; Woodhead, J. H.; Wilcox, K. S.; Stables, J. P.; Kupferberg, H. J.; Wolf, H. H. In *Antiepileptic Drugs*; Levy, R. H., Mattson, R. H., Meldrum, B. S., Perruca, E., Eds., 5th ed.; Lippincott, Williams and Wilkins: Philadelphia, PA, 2002; pp 36–48.
35. Swinyard, E. A. *Epilepsia* **1969**, *10*, 107.
36. Salome, C.; Salome-Grosjean, E.; Park, K. D.; Morieux, P.; Swendiman, R.; DeMarco, E.; Stables, J. P.; Kohn, H. *J. Med. Chem.* **2010**, *53*, 1288.
37. Errington, A. C.; Stoehr, T.; Heers, A. C.; Lees, G. *Mol. Pharmacol.* **2008**, *73*, 157.
38. Sheets, P. L.; Heers, C.; Stoehr, T.; Cummins, T. R. *J. Pharm. Exp. Ther.* **2008**, *326*, 88.
39. Lee, H.; Park, K. D.; Yang, X.-F.; Dustrude, E. T.; Wilson, S. M.; Khanna, R.; Kohn, H. *J. Med. Chem.* **2013**, *56*, 5931.
40. Goldin, A. L. *Annu. Rev. Physiol.* **2001**, *63*, 871.
41. Wang, H.; Oxford, G. S. *J. Neurophysiol.* **2000**, *84*, 2888.
42. Wang, Y.; Brittain, J. M.; Jarecki, B. W.; Park, K. D.; Wilson, S. M.; Wang, B.; Hale, R.; Meroueh, S. O.; Cummins, T. R.; Khanna, R. *J. Biol. Chem.* **2010**, *285*, 25296.
43. Hodgkin, A. L.; Huxley, A. F. *J. Physiol.* **1952**, *116*, 497.
44. Rudy, B. *J. Physiol.* **1978**, *283*, 1.
45. Bean, B. P. *Nat. Rev. Neurosci.* **2007**, *8*, 451.
46. Do, M. T. H.; Bean, B. P. *Neuron* **2003**, *39*, 109.
47. Vilin, Y. Y.; Ruben, P. C. *Cell Biochem. Biophys.* **2001**, *35*, 171.
48. Errington, A. C.; Stohr, T.; Lees, G. *Curr. Top. Med. Chem.* **2005**, *5*, 15.
49. Wang, Y.; Park, K. D.; Salome, C.; Wilson, S. M.; Stables, J. P.; Liu, R.; Khanna, R.; Kohn, H. *ACS Chem. Neurosci.* **2011**, *2*, 90.
50. Errington, A. C.; Stohr, T.; Heers, C.; Lees, G. *Mol. Pharmacol.* **2008**, *73*, 157.
51. Catterall, W. A. *Novartis Found. Symp.* **2002**, *241*, 206. discussion 218.
52. Rowley, N. M.; White, H. S. *Epilepsy Res.*. **2010**, *92*, 163.
53. Morimoto, K.; Fahnestock, M.; Racine, R. J. *Prog. Neurobiol.* **2004**, *73*, 1.
54. Lothman, E. W.; Williamson, J. M. *Brain Res.* **1994**, *649*, 71.
55. White, H. S. *Epilepsia* **2003**, *44*, 2.
56. UNC's NIMH Psychoactive Drug Screening Program: http://pdsp.med.unc.edu.
57. Bialer, M.; Johannessen, S. I.; Kupferberg, H. J.; Levy, R. H.; Loiseau, P.; Percucca, E. *Epilepsy Res.*. **2002**, *51*, 31.
58. Brittain, J. M.; Piekarz, A. D.; Wang, Y.; Kondo, T.; Cummins, T. R.; Khanna, R. *J. Biol. Chem.* **2009**, *284*, 31375.
59. Brittain, J. M.; Wang, Y.; Eruvwetere, O.; Khanna, R. *FEBS Lett.* **2012**, *586*, 3813.